

# Radiation-Induced Liver Injury: An Overview

Jing Sun<sup>1,\*</sup>, Hao-ran Lu<sup>1,\*</sup>, Jian-hui Wu<sup>2,\*</sup>, Dong Li<sup>1,\*</sup>, Tao Zhang<sup>1</sup>, Xue-zhang Duan<sup>1</sup>

<sup>1</sup>Department of Radiation Oncology, Senior Department of Oncology, The Fifth Medical Center of PLA General Hospital, Beijing, People's Republic of China; <sup>2</sup>Medical School, Chinese PLA General Hospital, Beijing, People's Republic of China

\*These authors contributed equally to this work

Correspondence: Xue-zhang Duan; Tao Zhang, Department of Radiation Oncology, Senior Department of Oncology, The Fifth Medical Center of PLA General Hospital, No. 100 Xi Si Huan Middle Road, Fengtai District, Beijing, 100039, People's Republic of China, Tel +8613621386161; +86 13641304338, Email duanxuezhang@301hospital.com.cn; 13641304338@126.com

**Abstract:** Radiation therapy is one of the main methods of tumor treatment, with over 50% of patients opting for it during treatment. The optimal regimen of radiation therapy aims to increase the dose in the target area while decreasing the dose in normal tissue. Radiotherapy for liver tumors has seen significant development in recent years. Despite the technological progress and improved accuracy of radiotherapy, the path of radiation reaching the target area still passes through normal tissues. Although there is tolerance doses as a reference parameter for normal liver exposure in planning, radiation damage still occurs. In addition, when combination of radiation therapy with chemotherapy, targeted therapy and immunotherapy has been widely used in recent years, the occurrence of RILD still affects the implementation of other treatment programs. In this review, latest research results of RILD are discussed to better understand the mechanism and provide research directions for optimizing radiotherapy.

**Keywords:** radiation-induced liver injury, radiation therapy, tolerance doses, normal tissue toxicity, radiotherapy optimization

## Introduction

According to global cancer statistics, there were nearly 20 million new cases of cancer in 2022, and 9.7 million deaths from cancer. In addition to the most common lung cancer and female breast cancer, colorectal cancer, prostate cancer, stomach cancer and liver cancer are the main types of cancer with high incidence and/or high mortality.<sup>1</sup> Radiation therapy plays an important role in the process of tumor treatment. More than 50% of cancer patients received radiation therapy, benefiting from both radical and palliative treatment effects.<sup>2</sup> Although current precision radiotherapy, such as intensity-modulated radiotherapy (IMRT) and volumetric modulated arc therapy (VMAT), stereotactic body radiation therapy (SBRT), radioembolization, etc, has optimized the dose to organs at risk (OARs) to the greatest extent, normal tissue damage by radiation remains one of the important factors affecting the therapeutic effect. Radiation induced liver injury (RILD) is not only the biggest obstacle to liver tumor radiotherapy, but also an important indicator to consider the dose of abdominal radiotherapy. Exploring the mechanism of RILD and its intervention lays the foundation for prevention and following treatment. Therefore, with RILD as the focus, the review discusses its molecular mechanisms and common interventions in recent years.

## Diagnosis Criteria of RILD

There are two types of RILD, classic RILD and non-classic RILD. Classic RILD manifested as anicteric hepatomegaly, ascites, elevated alkaline phosphatase ( $>2 \times$  ULN [upper limit of normal] or baseline value), typically occurring 2 weeks to 3 months after therapy.<sup>3</sup> Non-classic RILD is identified when meeting one of the following conditions: 1) Elevated liver transaminases  $>5$  ULN; 2) CTCAE Grade 4 with  $>5$  ULN baseline values within 3 months after completion of radiotherapy; 3) Child-Pugh score increasing  $\geq 2$  scores. The conditions above were all in the absence of classic RILD, typically occurring one week to three months after therapy.<sup>4</sup>

In clinical practice, it is often challenging to differentiate between liver dysfunction caused by disease progression and RILD, particularly in patients with advanced disease or pre-existing poor liver function. The effective liver volume would shrink as a result of tumor progression, failing to compensate for normal liver function, thus leading to abnormal liver function. In addition, tumor invasion of the portal vein may lead to portal vein tumor thrombus (PVTT), causing obstruction in normal liver blood supply, which also induces abnormal liver function. Moreover, for patients who take oral antiviral drugs to treat viral hepatitis and achieve negative in virus tests, there is a possibility of viral reactivation after radiotherapy, which can also result in abnormal liver function and interfere with the diagnosis of RILD.

## Pathological Changes in RILD

The mechanism of RILD is complex, and the main pathological changes are a combination of endothelial cell edema, terminal hepatic venule narrowing, sinusoidal congestion, zonal parenchymal atrophy, accumulation of collagen in the subendothelial space (space of Disse) and secondary hepatocyte necrosis.<sup>4,5</sup> Typical pathological manifestation of RILD includes damage to hepatocytes, hepatic stellate cells (HSCs), Kupffer cells (KCs) and other hepatocytes.<sup>6</sup> Oxidative stress, hepatocyte senescence, apoptosis, and fibrosis all play important roles in the development of RILD.<sup>7,8</sup>

Radiation directly damages hepatocytes through oxidative stress and inflammatory responses, initiating a cascade of liver injury. This injury is further amplified by the activation of Kupffer cells (KCs) and the recruitment of circulating immune cells, which exacerbate inflammation and fibrosis.<sup>9</sup> As specialized liver macrophages, KCs originate from blood monocytes adhering to hepatic sinusoids and function to clear foreign particles and damaged erythrocytes via phagocytosis. Following irradiation, KCs secrete tumor necrosis factor- $\alpha$  (TNF- $\alpha$ ) in a dose-dependent manner, which promotes hepatocyte apoptosis when co-cultured with irradiated hepatocytes.<sup>10</sup> In vivo studies in rats demonstrate that KC inhibition reduces pro-inflammatory cytokine production (IL-1 $\beta$ , IL-6, IFN, and TNF- $\alpha$ ), thereby alleviating acute RILD.<sup>11</sup> Additionally, selective KC inhibition mitigates radiation-induced SEC apoptosis, offering protection against RILD.<sup>12</sup> Concurrently, injured sinusoidal endothelial cells (SECs) undergo apoptosis and release TNF- $\alpha$ , further driving hepatocyte apoptosis and KC activation.<sup>9</sup> SEC dysfunction also leads to erythrocyte extravasation and fibrin deposition in central veins, contributing to sinusoidal obstruction.<sup>9</sup> Notably, hepatocytes and SECs engage in reciprocal regulation through TLR4 and TNFR1 signaling pathways.<sup>13</sup> HSCs play a pivotal role in both classic and non-classic RILD, contributing not only to hepatocyte regeneration but also to the secretion of lipoproteins, growth factors, and cytokines that modulate inflammation and fibrosis.<sup>9,10,13,14</sup> Their activation is a critical step in the development of radiation-induced liver fibrosis (RILF), a hallmark of late-stage RILD. Activated KCs secrete transforming growth factor- $\beta$  (TGF- $\beta$ ), the primary profibrogenic cytokine, which drives HSC activation and subsequent fibrogenesis<sup>9</sup> (Figure 1).

## Radiological Changes in RILD

The hepatomegaly and ascites as diagnostic criteria of RILD can be observed in imaging tests. After focal irradiation of the liver, the irradiated hepatic parenchyma, compared with the surrounding non-irradiated hepatic parenchyma, typically shows hypo-attenuation on plain CT and hyper-attenuation on contrast-enhanced CT.<sup>6</sup> Tomoki Kimura et al<sup>15</sup> reported that dynamic CT imaging can be classified into 3 types after stereotactic body radiotherapy: type 1, hyper-density in all enhanced phases; type 2, hypodensity in arterial and portal phases; type 3, iso-density in all enhanced phases. Further analysis found that half of the type 2 or 3 findings significantly changed to type 1, particularly in patients belonging to Child-Pugh classification A. After 3–6 months, patients of Child-Pugh B classification mainly presented the type 3 pattern. To sum up, dynamic CT results could be classified into 3 patterns and those of Child-Pugh A patients mostly changed over time into the enhancement group (type 1). Irradiated liver parenchyma area in magnetic resonance (MR) typically exhibits a sharply defined wide band of hypo-intensity on T1-weighted images (T1WI), hyperintensity on T2WIs, slight hyperintensity on diffusion-weighted imaging (DWI), with low apparent diffusion coefficient (ADC) values corresponding to the radiation port.<sup>16,17</sup> Poonam Yadav et al<sup>18</sup> transferred 10 Gy–70 Gy treatment isodose lines in increments of 1 Gy from the planning scans to the follow-up diagnostic MR scans and they found that a median dose of 35 Gy correlated most closely with the visible RILD. It is necessary to distinguish between RILD and metastasis in CT and MR imaging,<sup>19</sup> as well as the uptake and accumulation of F-18-fluorodeoxyglucose (18F-FDG) and F-18-labeled fibroblast-activation protein inhibitor (18F-FAPI) in PET/CT imaging that are caused by RILD or other conditions in

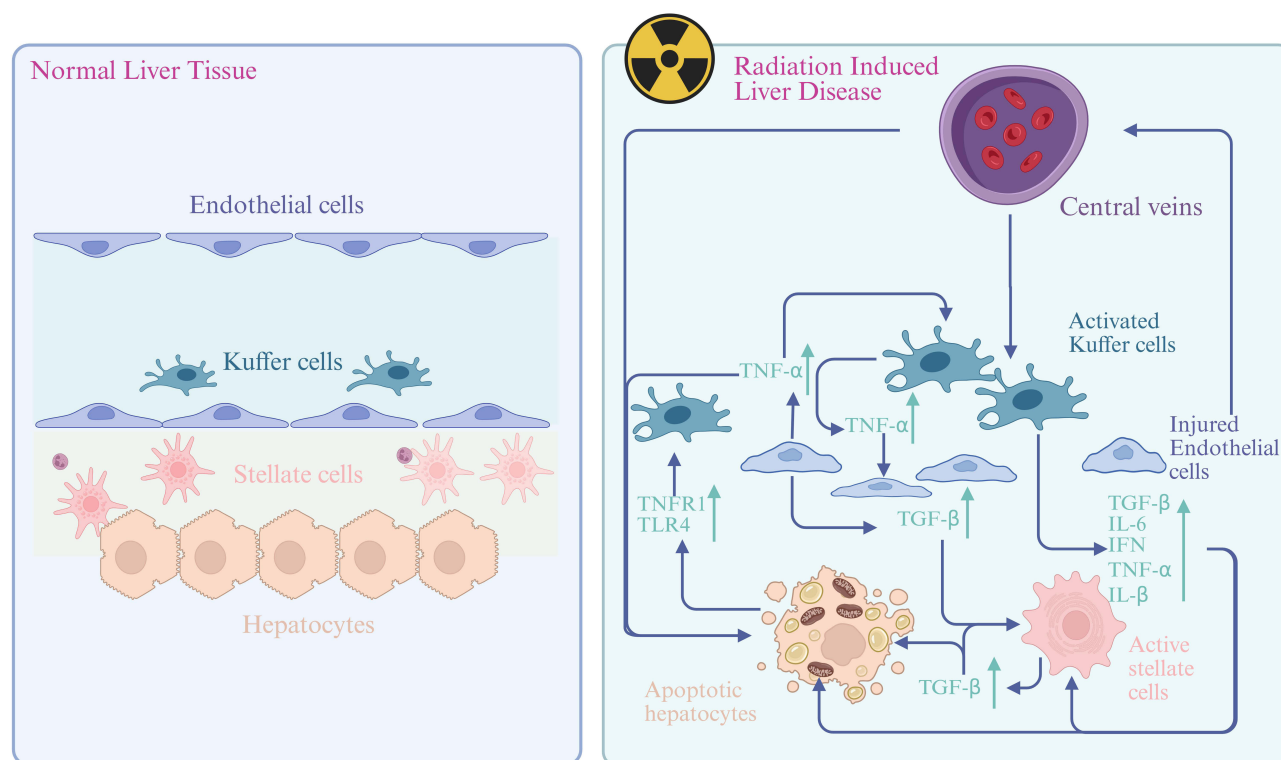


**Figure 1** Radiation-induced cellular changes and inflammatory crosstalk in the liver.

clinic settings.<sup>20,21</sup> Enoch Chang et al<sup>22</sup> conjectured that liver-directed radiotherapy can be safely delivered at high doses when incorporating functional SPECT into the radiation treatment planning process, which may enable sparing of lower volumes of liver than traditionally accepted in patients with preserved liver function.

We performed gadoxetic acid-enhanced MRI (EOB-MRI) on 32 post-treatment patients, and the imaging findings of the targeted area and surrounding areas before and after radiation therapy were shown in Figure 2.

## Related Research of RILD

Ionizing radiation can induce oxidative damage to DNA, lipids, proteins, and metabolites in both tumor and normal cells. The accumulation of DNA damage and reactive oxygen species (ROS) can trigger cell death via various mechanisms, such as apoptosis, necrosis, necroptosis and ferroptosis. Additionally, ionizing radiation can lead to senescence and autophagy.<sup>23</sup> In recent years, several fundamental studies on RILD have been conducted, encompassing in-vitro cell experiments and in-vivo animal studies (Table 1), with the RILD modeling methods detailed in Table 2. The results revealed that RILD is a complex process that can cause changes in a variety of signal pathways. In addition, some in-vivo animal studies also found that hepatobiliary secretion of bile acids<sup>24</sup> and fibrinogen-like 1(FGL1) upregulation<sup>25</sup> may serve as a potential biomarker for acute and sub-acute radiation exposure to the liver. In the early stages, our research team successfully established a RILD model using New Zealand white rabbits and SD rats (Figure 3), irradiated with a CyberKnife system. The success of modeling provided a guarantee for later mechanism research.

In recent years, numerous studies on RILD have initially identified differences in clinical samples and subsequently validated these findings through animal experiments to enhance the objectivity of the research. Zeng ZC et al<sup>39,40</sup> found that compared with non-irradiated samples, expression of STING and interleukin-1 $\beta$  in kupffer cells (KCs) and non-parenchymal cells (NPCs) increased in clinical human normal liver tissue samples collected after irradiation. Targeting and inhibiting STING alleviated irradiation-induced liver injury in mice, indicating its therapeutic potential in RILD. Su TS et al<sup>41</sup> reported that Akt/mTOR participates in liver regeneration after RILD in human specimens, then they found that the Akt activator-carbamazepine and mTOR inhibitor-temsirolimus both could enhance liver regeneration in rats.

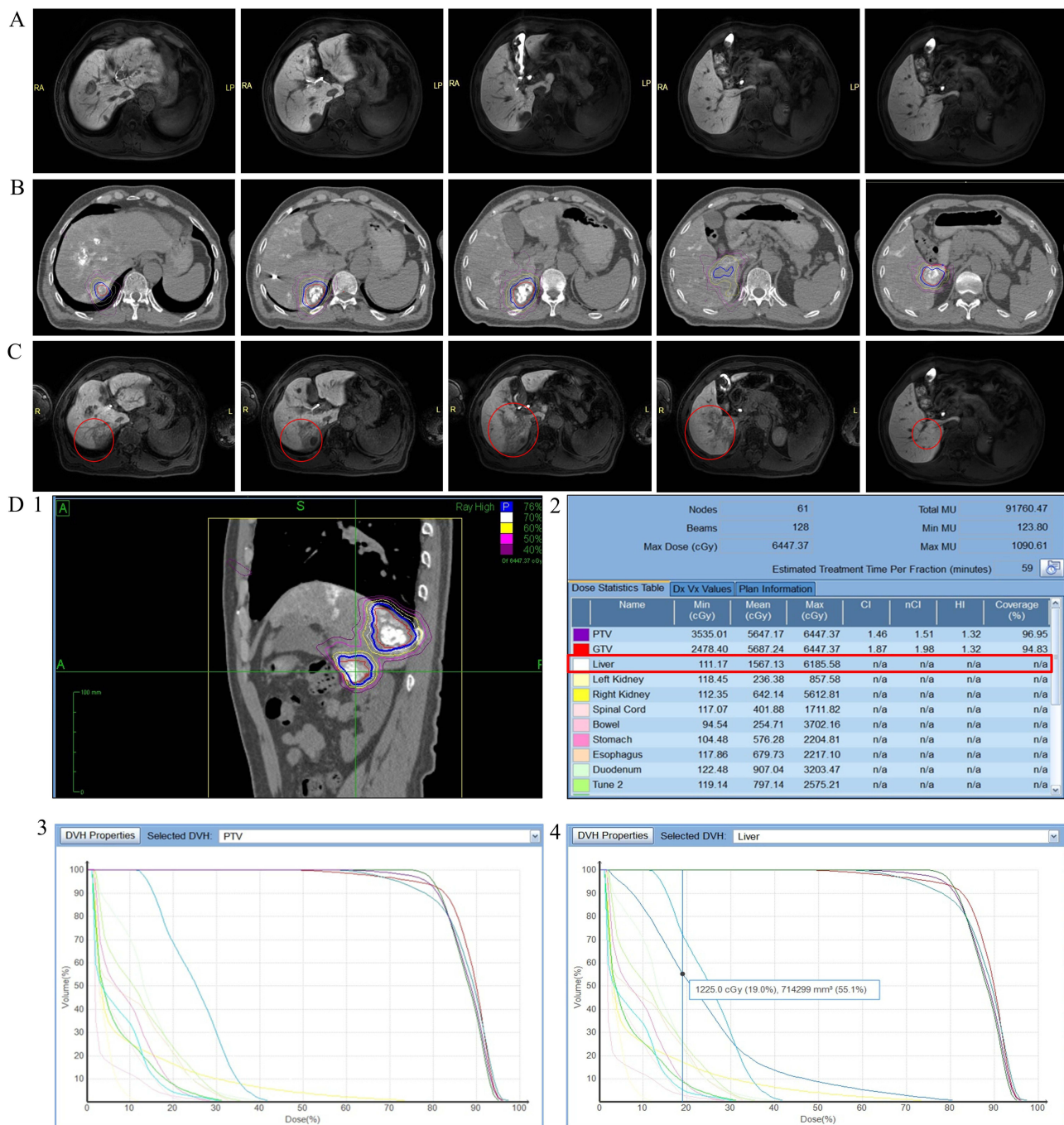


**Figure 2** Radiation-induced liver injury on gadoxetic acid-enhanced MRI (EOB-MRI, 18–20min) at 3 months post-radiotherapy along with treatment planning details, where (A) shows pretreatment liver MRI, (B) displays the radiation dose distribution, (C) presents the hepatobiliary phase (18–20 min) of MRI. The hypointense regions within the red circles correspond to the irradiated areas, and (D) presents treatment planning parameters including prescription isodose distribution (D1), Liver dose-volume metrics (D2; mean dose of 1567.13cGy, maximum dose of 6185.58cGy, and minimum dose of 111.17cGy within the red box), and dose-volume histogram (DVH, D3), with 714 mm<sup>3</sup> of liver volume receiving 12.25 Gy radiation dose (D4).

### Clinical Influence Factors of RILD

Some researchers have investigated parameters such as radiotherapy dose using various techniques, aiming to identify high-risk factors and reduce the incidence of RILD. The Child-Pugh classification has been widely recognized as a significant factor influencing the development of RILD.<sup>42,43</sup> Clinical studies on radiation therapy for liver cancer and corresponding incidence of RILD over the past five years are shown in Table 3. One of our previous studies

**Table 1** In-vitro and in-vivo Studies of RILD

Study	Signaling Pathway	Intervening Measure	Functioning Cells/ Animal Tests
Liu Y et al <sup>26</sup> Yuhan C et al <sup>27,28</sup>	AdipoRon/AdipoR1/ AMPK $\alpha$ MicroRNA-146a-5p/TLR4	AdipoRon 1.2 mg/kg via tail vein injections Qod	Hepatocytes (HHL-5) HSCs and hepatocytes Male C3H/HeN mice
Lei Xiao et al <sup>29</sup>	PI3K/Akt signaling pathway		HSCs (HSC-T6) Male SD rats
Wei Li et al <sup>30</sup> Liu Q et al <sup>31</sup>	NF- $\kappa$ B signaling pathway Nrf2/ HO-1	Curcumina via intragastric administrated dose of 30 mg/kg Qd Phycocyanin	SD mouse C57BL/6 mice
Shereen M Shedid et al <sup>7</sup> Nicolas Melin et al <sup>32</sup>	p53 pathway	Betaine (400mg/kg/d, oral), after the first radiation dose	Male Wistar albino rats BALB/c female mice (8 weeks old)
Bing-Shen Huang et al <sup>33</sup>	KLF4 signaling pathway	BPC157: In-vitro cell tests: 1 $\mu$ g/mL BPC157; In-vivo animal tests: BPC157 (10 $\mu$ g/kg, 5 mL/kg, oral)	Rat liver clone 9 cells C57BL/6 mice
Rania A Gawish et al <sup>34</sup> Li HY et al <sup>35</sup>	JAK/STAT pathway	Ferulic acid (50mg/kg, oral for seven days). <i>p</i> -coumaric acid (100 mg/kg) for 4 consecutive days	Male rats C57BL/6 male mice
Asmaa A Hassan et al <sup>36</sup>	TNF- $\alpha$ /NF- $\kappa$ B signaling pathway, Pro- Fibrotic Factor TGF- $\beta$ 1	Mangosteen (500 mg/kg, oral)	Male Wistar albino rats

**Table 2** Experimental Methods for Establishing RILD Models

	Animal Species	RILD Modeling Scheme
Shereen M Shedid <sup>7</sup>	Male Wistar albino rats (150–180g)	The whole-body was exposed to 3 fractions of 3 Gy/wk (total dose of 9Gy)
Nicolas Melin <sup>32</sup> Bing-Shen Huang <sup>33</sup>	BALB/c female mice of 6 weeks C57BL/6 mice of 7 weeks (20–25g)	1% of the liver volume received the full 50 Gy dose, IGRT The whole abdomen (from xyphoid to pubis) and dose was 12Gy/1f
Li W et al <sup>30</sup>	Sprague-Dawley (SD) (180–220 g)	The lead block covered the left lung and mediastinum, 12Gy/3f, F992AT type 500 mA X-ray
Rania A Gawish et al <sup>34</sup>	Adult male rats (220–250 g)	The whole-body gamma irradiation of 6Gy by Cesium-137 source
Li HY et al <sup>35</sup> Kristoffer Kjergaard et al <sup>24</sup>	C57BL/6 male mice Göttingen minipigs	The total body X-ray (Simens company, Munich, Germany) irradiation of a single dose of 4 Gy The whole-liver, 14 Gy/1f, SBRT (Varian, Trilogy)
Asmaa A Hassan et al <sup>36</sup> Na-Kyung Han <sup>25</sup>	Wistar albino rats (150 $\pm$ 20 gm) Male BALB/c mice (18.2 $\pm$ 2.1 g)	The whole-body gamma irradiation of 6Gy by Cesium-137 source 30 Gy of liver IR encompassing over 80% of the liver volume, XRAD-SmART
Lu JK <sup>37</sup> Cagin YF <sup>38</sup>	Male Kunming mice of 6 weeks Female Wistar albino rats (220g)	The whole-body irradiation of 4 Gy at 1Gy/min by a <sup>60</sup> Co irradiator A single 800 cGy dose of radiation to the entire abdomen

demonstrated that platelet count is a critical factor in predicting RILD prognosis.<sup>44</sup> Reflecting the degree of liver cirrhosis, platelet count may have similar impact as Child-Pugh classification on RILD. Various studies have indicated that prolonged pre-treatment prothrombin time, hepatitis virus positivity, a higher number of tumors, tumors located at the hepatic hilum, elevated albumin-bilirubin scores, and increased body mass index are all contributing factors to RILD.<sup>42,45–48</sup> In addition to the well-known effective liver volume  $\geq 700$ mL, several planning parameters have been reported as related to the occurrence of RILD, including the mean dose on normal liver, V15, V25, V30, etc.<sup>42,43,45</sup>

In Asia, many patients with liver cancer have cirrhosis due to hepatitis B or C infection, and their liver cell function differs significantly from that of non-cirrhotic patients. However, until now, there has been no liver tolerance dose standard specifically for patients with cirrhosis. Therefore, for these patients with an effective liver volume of around 700cc, clinical experience is very important when designing radiation therapy plans. Our clinical observations revealed that in HCC patients treated with SBRT, with an effective normal liver volume of 700cc and a maximum BED<sub>10</sub> of 102.6Gy (DT: 54Gy/6f), the primary factors influencing RILD were baseline liver function parameters, including platelet count, white blood cell count, and albumin levels (Clinical Trials NCT: 03295500, other results are not shown here). Our

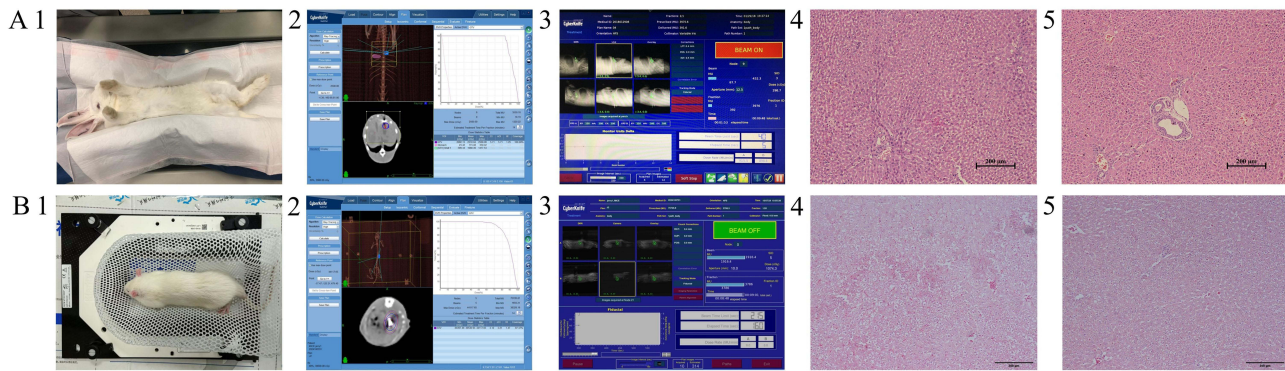


**Figure 3** Prior to radiotherapy, fiducial markers were percutaneously implanted into the liver of New Zealand white rabbits/SD mouse under CT guidance. **(A)** RILD model using New Zealand white rabbits. A1, immobilization achieved using vacuum cushions. A2, followed by dose delivery. A3, Histopathological evaluation compared irradiated liver tissue. A4, with untreated controls (A5), through HE staining (200× magnification). Pre-radiotherapy liver function tests showed ALP 25 IU/L, AST 27 IU/L, and ALT 28 IU/L, which increased to 357 IU/L (ALP), 426 IU/L (AST), and 228 IU/L (ALT) post-radiotherapy, indicating significant hepatic injury. **(B)** RILD model using SD mouse. B1, immobilization achieved using thermoplastic mask immobilization. B2, treatment planning was conducted using CyberKnife Multiplan system (version 4.0.2). B3, followed by dose delivery. B4, histopathological evaluation compared irradiated liver tissue with untreated controls (B5) through HE staining (200× magnification). Pre-radiotherapy liver function tests showed ALP 72 IU/L, AST 32 IU/L, and ALT 45 IU/L, which increased to 223 IU/L (ALP), 222 IU/L (AST), and 126 IU/L (ALT) post-radiotherapy, indicating significant hepatic injury.

team referred AAPM TG-101,<sup>61</sup> Timmerman’s Standard<sup>62</sup> and QUANTEC<sup>63</sup> for liver radiation therapy tolerance when treating liver tumors with SBRT and IMRT, without additional classification of liver function based on Child-Pugh scores. Our center has been treating liver tumors with radiotherapy for fifteen years with an acceptable incidence rate of RILD and no deaths due to RILD. Matthew M cousins et al<sup>64</sup> found that elevated plasma soluble TNFα receptor (sTNFR1) was associated with liver injury after radiotherapy, suggesting that elevated inflammatory cytokine activity was a predictor of RILD.

**Table 3** Incidence of Radiation-Induced Liver Disease in Clinical Practices

Study	Radiation Technique	Number of Patients	Dose Schedule	RILD
Marco Lorenzo Bonù, 2024 <sup>49</sup>	Protons or Photons	178 patients (213 lesions)	Photon: 60 Gy/3 fractions; Proton: 58–67.5 Gy/15f	Proton: 1 case; Photon: 1 case.
Ahmed Allam Mohamed, 2024 <sup>50</sup>	SBRT	52 HCC patients (a total of 62 lesions)	40 (24–66) Gy/5 (3–12) fx	4 cases were diagnosed with non-classic RILD
Zhang RJ, 2023 <sup>51</sup>	IMRT or VMAT	96 unresectable HCC: 30 cases underwent RT + PDI;66 patients underwent RT alone. After PSM, 30 cases were in each group.	51.0 Gy (47.5–60.0 Gy), 3.0 Gy (2.4–4.0 Gy) per fraction	7 patients were diagnosed with non-classic RILD in each group after PSM
Rodney Cheng-En Hsieh, 2023 <sup>52</sup>	Protons or Photons	159 HCC patients (>5cm)	Proton: 72.6 CGE <sup>3</sup> /22f for central tumors and 66 CGE/10f for peripheral tumors; Photon: 50, 45 or 40 Gy/5f.	Proton: 12 cases (11.4%); Photon: 16 cases (29.6%)
Won Il Jang, 2023 <sup>53</sup>	IMRT	1755 HCC patients (most patients had advanced-stage HCC and combined treatment)	51 Gy (42–62 Gy), 1.8–6Gy per fraction	The occurrence rates of classic RILD, non-classic RILD and hepatic toxicity ≥ grade 3 were 2%, 4%, and 4%, respectively.
Karl Bordeau, 2023 <sup>54</sup>	MRgRT	56 primary liver tumors (seventy-two lesions)	50Gy/5f	None
Chen Bo, 2021 <sup>55</sup>	IMRT	76 eligible patients who underwent narrow-margin resection	50-60 Gy/25-30f; Mean dose of whole liver ≤24 Gy	None

(Continued)

**Table 3** (Continued).

Study	Radiation Technique	Number of Patients	Dose Schedule	RILD
Hiromitsu, 2021 <sup>56</sup>	Image-Guided Proton Therapy	71 elderly patients with HCC	Peripheral tumor 66Gy/10f (forty-seven cases); Central tumor 72.6Gy/22f (twenty- four cases).	1 case was diagnosed with Grade 3 RILD
Ying-Fu Wang, 2021 <sup>57</sup>	CyberKnife-SBRT	14 advanced HCC patients (a total of 25 HCC lesions)	28-60Gy/4-5f	1 case was diagnosed with non-classic RILD
Munire Abulimiti, 2021 <sup>58</sup>	IMRT	82 HCC patients: 36 cases underwent IMRT+ sorafenib; 46 cases underwent IMRT alone.	40-62.5 Gy, 2–2.5 Gy per fraction	None
Won Il 2020 <sup>59</sup>	SBRT	74 unresectable HCC	45Gy-60Gy/3f	1 case was diagnosed with Grade 3 RILD
Stephanie K. Schaub, 2020 <sup>60</sup>	Intensity-modulated proton therapy (IMPT)	25 HCC patients with large tumors near OARs	Median mean and minimum dose delivered to the GTV was 64.0 Gy (54.3–69.6) and 45.1 Gy (33.4–67.7), respectively. Median mean dose to liver minus GTV was 15.0 Gy (8.2–19.6).	2 cases were diagnosed with RILD

**Note:** <sup>a</sup>CGE: Relative biologic effectiveness was set to 1.1 for cobalt Gy equivalent.

## Future Prospects of RILD

In conclusion, RILD is a major limiting factor in radiation therapy for abdominal tumors, especially liver cancer. Although the diagnostic criteria for RILD are well-defined, it remains essential to differentiate RILD from liver dysfunction caused by tumor progression or viral hepatitis reactivation in advanced-stage patients. Research utilizing in-vitro cell experiments and in-vivo animal models provides an effective approach to elucidating the underlying mechanisms of RILD. For patients with advanced liver tumors, the emergence of targeted and immunotherapy has provided them with more treatment options, but it has also concurrently increased the risk of liver injury. As the current treatment paradigm for most patients with advanced hepatocellular carcinoma involves a combination of local therapy and systemic anti-tumor therapy, greater emphasis must be placed on the potential for the co-occurrence of drug-induced liver injury (DILI) and RILD. Although advances in radiotherapy have effectively lowered radiation exposure of liver and the risk of liver damage, fully understanding the mechanism of RILD and developing new therapeutic agents to reduce RILD are essential to improve patients' survival rates.

## Ethics Approval Statement

The Ethics Committee Board of the Fifth Medical Center of PLA General Hospital approved this review and waived the requirement for patient consent (Case in [Figure 2](#)). This study was conducted in compliance with the Declaration of Helsinki. We confirm that all procedures strictly adhered to relevant laws and regulations, and no patient personal information was disclosed to unauthorized individuals or organizations, ensuring the confidentiality and security of patient data.

All animal experiments were approved by the Ethics Committee Board of the Fifth Medical Center of PLA General Hospital and performed in accordance with the National Institutes of Health (NIH) Guide for the Care and Use of Laboratory Animals. Animals were housed in a controlled environment with a 12-hour light/dark cycle and provided with ad libitum access to food and water. Surgical procedures were performed under anesthesia, and postoperative analgesia was administered to minimize pain and distress. Every effort was made to reduce the number of animals used while maintaining the statistical validity of the results.

## Author Contributions

All authors made a significant contribution to the work reported, whether that is in the conception, study design, execution, acquisition of data, analysis and interpretation, or in all these areas; took part in drafting, revising or critically

reviewing the article; gave final approval of the version to be published; have agreed on the journal to which the article has been submitted; and agree to be accountable for all aspects of the work.

## Funding

This review was supported by the following grants: National Natural Science Foundation of China (Grant Number: 82202968, Jing Sun.) and National Natural Science Foundation of China (Grant Number: 81972856, Xue-zhang Duan).

## Disclosure

The authors declare that they have no competing interests.

## References

1. Bray F, Laversanne M, Sung H, et al. Global cancer statistics 2022: GLOBOCAN estimates of incidence and mortality worldwide for 36 cancers in 185 countries. *CA Cancer J Clin.* 2024;74:229–263. doi:10.3322/caac.21834
2. De Ruyscher D, Niedermann G, Burnet NG, Siva S, Anne WML, Hegi-Johnson F. Radiotherapy toxicity. *Nat Rev Dis Primers.* 2019;5:1.
3. Lawrence TS, Robertson JM, Anscher MS, Jirtle RL, Ensminger WD, Fajardo LF. Hepatic toxicity resulting from cancer treatment. *Int J Radiat Oncol Biol Phys.* 1995;31(5):1237–1248. doi:10.1016/0360-3016(94)00418-K
4. Charlie C, Brian D, Dawson LA, et al. Radiation-associated liver injury. *Int J Radiat Oncol Biol Phys.* 2010;76:1.
5. Reed GB, Cox AJ. The human liver after radiation injury. A form of veno-occlusive disease. *Am J Pathol.* 1966;48:597–611.
6. Takamatsu S, Kozaka K, Kobayashi S, et al. Pathology and images of radiation-induced hepatitis: a review article. *Jpn J Radiol.* 2018;36:241–256. doi:10.1007/s11604-018-0728-1
7. Shedid SM, Abdel-Magied N, Saada HN. Role of betaine in liver injury induced by the exposure to ionizing radiation. *Environ Toxicol.* 2019;34:123–130. doi:10.1002/tox.22664
8. Zhu W, Zhang X, Mengli Y, Lin B, Chaohui Y. Radiation-induced liver injury and hepatocyte senescence. *Cell Death Discov.* 2021;7. doi:10.1038/s41420-021-00634-6
9. Kim J, Jung Y. Radiation-induced liver disease: current understanding and future perspectives. *Exp Mol Med.* 2017;49:e359. doi:10.1038/emm.2017.85
10. Christiansen H, Saile B, Neubauer-Saile K, et al. Irradiation leads to susceptibility of hepatocytes to TNF-alpha mediated apoptosis. *Radiation Oncol.* 2004;72:291–296. doi:10.1016/j.radonc.2004.07.001
11. Shi-Suo D, Qiang M, Zeng Z-C, et al. Inactivation of kupffer cells by gadolinium chloride protects murine liver from radiation-induced apoptosis. *Int J Radiat Oncol Biol Phys.* 2010;76:1225–1234. doi:10.1016/j.ijrobp.2009.09.063
12. Chen YX, Zeng ZC, Sun J, Zhang ZY, Zeng HY, Hu WX. Radioprotective effect of kupffer cell depletion on hepatic sinusoidal endothelial cells. *Radiation Res.* 2015;183:563–570. doi:10.1667/RR13869.1
13. Zhou P, Deng Y, Sun Y, Dehua W, Chen Y. Radiation-sensitive circRNA hsa\_circ\_0096498 inhibits radiation-induced liver fibrosis by suppressing EIF4A3 nuclear translocation to decrease CDC42 expression in hepatic stellate cells. *J Transl Med.* 2024;22. doi:10.1186/s12967-024-05695-6
14. Sempoux C, Horsmans Y, Geubel A, et al. Severe radiation-induced liver disease following localized radiation therapy for biliopancreatic carcinoma: activation of hepatic stellate cells as an early event. *Hepatology.* 1997;1997:26.
15. Kimura T, Takahashi S, Takahashi I, et al. The time course of dynamic computed tomographic appearance of radiation injury to the cirrhotic liver following stereotactic body radiation therapy for hepatocellular carcinoma. *PLoS One.* 2015;10:e0125231. doi:10.1371/journal.pone.0125231
16. Yankelevitz DF, Knapp PH, Henschke CI, Nisce L, Yi Y, Cahill P. MR appearance of radiation hepatitis. *Clin Imaging.* 1992;16:89–92. doi:10.1016/0899-7071(92)90118-S
17. Park HJ, Kim SH, Jang KM, et al. Added value of diffusion-weighted MRI for evaluating viable tumor of hepatocellular carcinomas treated with radiotherapy in patients with chronic liver disease. *AJR.* 2014;202:92–101. doi:10.2214/AJR.12.10212
18. Yadav P, Kuczmaraska-Haas A, Musunuru HB, et al. Evaluating dose constraints for radiation induced liver damage following magnetic resonance image guided Stereotactic Body radiotherapy. *Phys Imaging Radiat Oncol.* 2021;17:91–94. doi:10.1016/j.phro.2021.01.009
19. Park H, Lee SY. Radiation-induced liver disease mimicking liver metastasis after low-dose hepatic irradiation during radiotherapy for gastric mucosa-assisted lymphoid tissue lymphoma: a case report. *Medicine.* 2024;103:e39191. doi:10.1097/MD.00000000000039191
20. Voncken FEM, Aleman BMP, van Dieren JM, et al. Radiation-induced liver injury mimicking liver metastases on FDG-PET-CT after chemoradiotherapy for esophageal cancer: a retrospective study and literature review. *Strahlenther Onkol.* 2018;194:156–163. doi:10.1007/s00066-017-1217-7
21. Zhang J, Jiang S, Zhang R, Zhang L. Increased 18F-FAPI uptake in radiation-induced liver injury. *Clin Nucl Med.* 2023;48(10):e474–e476. doi:10.1097/RLU.00000000000004801
22. Chang E, Wong FCL, Chasen BA, et al. Phase I trial of single-photon emission computed tomography-guided liver-directed radiotherapy for patients with low functional liver volume. *JNCI Cancer Spectr.* 2024;8. doi:10.1093/jncics/pkae037
23. Khodamoradi E, Hoseini-Ghahfarokhi M, Amini P, et al. Targets for protection and mitigation of radiation injury. *Cell Mol Life Sci.* 2020;77:3129–3159. doi:10.1007/s00018-020-03479-x
24. Kjærgaard K, Weber B, Alstrup AKO, et al. Hepatic regeneration following radiation-induced liver injury is associated with increased hepatobiliary secretion measured by PET in Göttingen minipigs. *Sci Rep.* 2020;10. doi:10.1038/s41598-020-67609-y
25. Han NK, Jung MG, Jeong YJ, et al. Plasma fibrinogen-like 1 as a potential biomarker for radiation-induced liver injury. *Cells.* 2019;8:1042. doi:10.3390/cells8091042
26. Liu Y, Yinfen X, Huilin J, et al. AdipoRon alleviates liver injury by protecting hepatocytes from mitochondrial damage caused by ionizing radiation. *Int J Mol Sci.* 2024;25:1.

27. Chen Y, Zhifeng W, Yuan B, Dong Y, Zhang L, Zeng Z. MicroRNA-146a-5p attenuates irradiation-induced and LPS-induced hepatic stellate cell activation and hepatocyte apoptosis through inhibition of TLR4 pathway. *Cell Death Dis.* 2018;9. doi:10.1038/s41419-017-0038-z
28. Chen Y, Yuan B, Chen G, et al. Circular RNA RSF1 promotes inflammatory and fibrotic phenotypes of irradiated hepatic stellate cell by modulating miR-146a-5p. *J Cell Physiol.* 2020;235:8270–8282. doi:10.1002/jcp.29483
29. Xiao L, Zhang H, Yang X, et al. Role of phosphatidylinositol 3-kinase signaling pathway in radiation-induced liver injury. *Kaohsiung J Med Sci.* 2020;36:990–997. doi:10.1002/kjm2.12279
30. Wei L, Jiang L, Xianzhou L, Liu X, Ling M. Curcumin protects radiation-induced liver damage in rats through the NF- $\kappa$ B signaling pathway. *BMC Complement Med Ther.* 2021;21:21. doi:10.1186/s12906-020-03187-w
31. Liu Q, Wenjun L, Qin S. Therapeutic effect of phycocyanin on acute liver oxidative damage caused by X-ray. *Biomed Pharmacother.* 2020;130:110553. doi:10.1016/j.biopha.2020.110553
32. Melin N, Yarahmadov T, Sanchez-Taltavull D, et al. A new mouse model of radiation-induced liver disease reveals mitochondrial dysfunction as an underlying fibrotic stimulus. *JHEP Rep.* 2022;2022:4.
33. Huang BS, Huang SC, Chen FH, et al. Pentadecapeptide BPC 157 efficiently reduces radiation-induced liver injury and lipid accumulation through Kruppel-like factor 4 upregulation both in vivo and in vitro. *Life Sci.* 2022;310:121072. doi:10.1016/j.lfs.2022.121072
34. Gawish RA, Samy EM, Aziz MM. Ferulic acid protects against gamma-radiation induced liver injury via regulating JAK/STAT/Nrf2 pathways. *Arch Biochem Biophys.* 2024;2024:753.
35. Yun-Hong L, Jiang-Xue W, Qian H, et al. Amelioration of radiation-induced liver damage by p-coumaric acid in mice. *Food Sci Biotechnol.* 2022;31:1315–1323. doi:10.1007/s10068-022-01118-8
36. Hassan AA, Moustafa EM, El-Khashab IH, Mansour SZ. Mangosteen hinders gamma radiation-mediated oxidative stress and liver injury by down-regulating TNF- $\alpha$ /NF- $\kappa$ B and pro-fibrotic factor TGF- $\beta$ 1 inducing inflammatory signaling. *Dose-Response.* 2021;19:15593258211025190. doi:10.1177/15593258211025190
37. Lu J, Chen C, Hao L, Zheng Z, Zhang N, Wang Z. MiRNA expression profile of ionizing radiation-induced liver injury in mouse using deep sequencing. *Cell Biol Int.* 2016;40:873–886. doi:10.1002/cbin.10627
38. Cagin YF, Parlakpınar H, Vardi N, Aksanyar S. Protective effects of apocynin against ionizing radiation-induced hepatotoxicity in rats. *Biotechnic Histochem.* 2022;97:228–235. doi:10.1080/10520295.2021.1936641
39. Wang B, Zhang Y, Niu H, et al. METTL3-Mediated STING upregulation and activation in kupffer cells contribute to radiation-induced liver disease via pyroptosis. *Int J Radiat Oncol Biol Phys.* 2023;119:219–233. doi:10.1016/j.ijrobp.2023.10.041
40. Shisuo D, Chen G, Yuan B, et al. DNA sensing and associated type I interferon signaling contributes to progression of radiation-induced liver injury. *Cell Mol Immunol.* 2020;18:1718–1728. doi:10.1038/s41423-020-0395-x
41. Su T, Zhao W, Qing L, Qiaoyuan W. Abstract 2417: liver regeneration after radiation therapy: clinical observations and a new rat model. *Cancer Res.* 2023;83. doi:10.1158/1538-7445.AM2023-2417
42. Qiaoyuan W, Wang Y, Wei Y, et al. Development and validation of a nomogram for radiation-induced hepatic toxicity after intensity modulated radiotherapy for hepatocellular carcinoma: a retrospective study. *Jpn J Clin Oncol.* 2024;54:699–707. doi:10.1093/jcco/hyae024
43. Hayashi K, Suzuki O, Wakisaka Y, et al. Prognostic analysis of radiation-induced liver damage following carbon-ion radiotherapy for hepatocellular carcinoma. *Radiat Oncol.* 2024;19. doi:10.1186/s13014-024-02444-3
44. Sun J, Wang Q, Hong Z-X, et al. Stereotactic body radiotherapy versus hepatic resection for hepatocellular carcinoma ( $\leq 5$  cm): a propensity score analysis. *Hepatol Int.* 2020;14:788–797. doi:10.1007/s12072-020-10088-0
45. Li JX, Zhang RJ, Qiu MQ, et al. Non-classic radiation-induced liver disease after intensity-modulated radiotherapy for Child-Pugh grade B patients with locally advanced hepatocellular carcinoma. *Radiat Oncol.* 2023;18:48. doi:10.1186/s13014-023-02232-5
46. Cheng JC-H, Jian-Kuen W, Lee PC-T, et al. Biologic susceptibility of hepatocellular carcinoma patients treated with radiotherapy to radiation-induced liver disease. *Int J Radiat Oncol Biol Phys.* 2004;60:1502–1509. doi:10.1016/j.ijrobp.2004.05.048
47. Uchinami Y, Katoh N, Suzuki R, et al. A study on predicting cases that would benefit from proton beam therapy in primary liver tumors of less than or equal to 5 cm based on the estimated incidence of hepatic toxicity. *Clin Transl Radiat Oncol.* 2022;35:70–75. doi:10.1016/j.ctro.2022.05.004
48. Yoshino Y, Suzuki G, Shiomi H, et al. Albumin-bilirubin score is a useful predictor of worsening liver reserve after stereotactic body radiation therapy in elderly Japanese patients with hepatocellular carcinoma. *J Radiat Res.* 2024;65:244–250. doi:10.1093/jrr/rrae006
49. Bonù ML, Nicosia L, Turkaj A, et al. High dose proton and photon-based radiation therapy for 213 liver lesions: a multi-institutional dosimetric comparison with a clinical perspective. *La Radiologia medica.* 2024;129:497–506. doi:10.1007/s11547-024-01788-w
50. Mohamed AA, Berres M-L, Bruners P, et al. Managing hepatocellular carcinoma across the stages: efficacy and outcomes of stereotactic body radiotherapy: a retrospective study. *Strahlenther Onkol.* 2024;200:715–724. doi:10.1007/s00066-024-02235-5
51. Zhang RJ, Zhou HM, Lu HY, et al. Radiotherapy plus anti-PD1 versus radiotherapy for hepatic toxicity in patients with hepatocellular carcinoma. *Radiat Oncol.* 2023;18:129. doi:10.1186/s13014-023-02309-1
52. Hsieh RC, Lee CH, Huang HC, et al. Clinical and dosimetric results of proton or photon radiation therapy for large ( $>5$  cm) hepatocellular carcinoma: a retrospective analysis. *Int J Radiat Oncol Biol Phys.* 2024;118:712–724. doi:10.1016/j.ijrobp.2023.09.049
53. Jang WI, Sunmi J, Moon JE, Bae SH, Park HC. The current evidence of intensity-modulated radiotherapy for hepatocellular carcinoma: a systematic review and meta-analysis. *Cancers.* 2023;15:4914. doi:10.3390/cancers15204914
54. Bordeau K, Michalet M, Dorion V, et al. A prospective registry study of stereotactic magnetic resonance guided radiotherapy (MRgRT) for primary liver tumors. *Radiother Oncol.* 2023;2023:189.
55. Chen B, Wu JX, Cheng SH, et al. Phase 2 study of adjuvant radiotherapy following narrow-margin hepatectomy in patients with HCC. *Hepatology.* 2021;74:2595–2604. doi:10.1002/hep.31993
56. Iwata H, Ogino H, Hattori Y, et al. A phase 2 study of image-guided proton therapy for operable or ablation-treatable primary hepatocellular carcinoma. *Int J Radiat Oncol Biol Phys.* 2021;111(1):117–126. doi:10.1016/j.ijrobp.2021.03.049
57. Wang Y-F, Dai Y-H, Lin C-S, et al. Clinical outcome and pathologic correlation of stereotactic body radiation therapy as a bridge to transplantation for advanced hepatocellular carcinoma: a case series. *Radiat Oncol.* 2021;16. doi:10.1186/s13014-020-01739-5
58. Abulimiti M, Zhenyu L, Wang H. Combination intensity-modulated radiotherapy and sorafenib improves outcomes in hepatocellular carcinoma with portal vein tumor thrombosis. *J Oncol.* 2021;2021:1–10. doi:10.1155/2021/9943683

59. Jang WI, Bae SH, Kim M-S, et al. A phase 2 multicenter study of stereotactic body radiotherapy for hepatocellular carcinoma: safety and efficacy. *Cancer*. 2019;2019:126.
60. Schaub Stephanie K, Bowen Stephen R, Nyflot Matthew J, Smith A. Intensity-modulated proton therapy using dose-painting pencil beam scanning for high-risk hepatocellular carcinoma. *J clin oncol*. 2020;38:558. doi:10.1200/JCO.2020.38.4\_suppl.558
61. Benedict SH, Yenice KM, Followill D, et al. Stereotactic body radiation therapy: the report of AAPM Task Group 101. *Med Phys*. 2010;37:4078–4101. doi:10.1118/1.3438081
62. Timmerman R. A Story of hypofractionation and the table on the wall. *Int J Radiat Oncol Biol Phys*. 2022;112:4–21. doi:10.1016/j.ijrobp.2021.09.027
63. Marks LB, Yorke ED, Jackson A, et al. Use of normal tissue complication probability models in the clinic. *Int J Radiat Oncol Biol Phys*. 2010;76:S10–S19. doi:10.1016/j.ijrobp.2009.07.1754
64. Cousins MM, Morris E, Maurino C, et al. TNFR1 and the TNF $\alpha$  axis as a targetable mediator of liver injury from stereotactic body radiation therapy. *Transl Oncol*. 2021;14:100950. doi:10.1016/j.tranon.2020.100950

Journal of Hepatocellular Carcinoma

Publish your work in this journal

The Journal of Hepatocellular Carcinoma is an international, peer-reviewed, open access journal that offers a platform for the dissemination and study of clinical, translational and basic research findings in this rapidly developing field. Development in areas including, but not limited to, epidemiology, vaccination, hepatitis therapy, pathology and molecular tumor classification and prognostication are all considered for publication. The manuscript management system is completely online and includes a very quick and fair peer-review system, which is all easy to use. Visit <http://www.dovepress.com/testimonials.php> to read real quotes from published authors.

Submit your manuscript here: <https://www.dovepress.com/journal-of-hepatocellular-carcinoma-journal>

Dovepress

Taylor & Francis Group